applied sciences

MDPI

Article

Bioinspired Divide-and-Conquer Design Methodology for a Multifunctional Contour of a Curved Lever

Jehyeok Kim, Junyoung Moon, Jaewook Ryu and Giuk Lee *

School of Mechanical Engineering, Chung-Ang University, Seoul 06974, Korea; michaeljhkim@cau.ac.kr (J.K.); mjyoung5@cau.ac.kr (J.M.); wodnr1958@cau.ac.kr (J.R.)
* Correspondence: giuklee@cau.ac.kr

Abstract: In this study, we propose a bioinspired design methodology for a multifunctional lever based on the morphological principle of the lever mechanism in the *Salvia pratensis* flower. The proposed divide-and-conquer contour design methodology does not treat a lever contour as a single curve that satisfies multiple functions. Rather, the lever contour combines partial contours to achieve its assigned subfunction. This approach can simplify the complex multifunctional problem in lever design. We include a case study of a lever utilized in a compact variable gravity compensator (CVGC) to explain the methodology in more detail. In the case study, four partial contours were designed to satisfy three types of functional requirements. The final design for the lever contour was manufactured and verified with visual measurement experiments. The experimental result shows that each partial contour successfully achieved its subfunctions.

Keywords: curved lever; lever design methodology; variable pivot of lever

check for updates

Citation: Kim, J.; Moon, J.; Ryu, J.; Lee, G. Bioinspired Divide-and-Conquer Design Methodology for a Multifunctional Contour of a Curved Lever. *Appl. Sci.* **2021**, *11*, 6015. https://doi.org/10.3390/app11136015

Academic Editors: TaeWon Seo, Dongwon Yun and Gwang-Pil Jung

Received: 28 May 2021
Accepted: 25 June 2021
Published: 28 June 2021

Publisher's Note: MDPI stays neutral with regard to jurisdictional claims in published maps and institutional affiliations.

Copyright: © 2021 by the authors. Licensee MDPI, Basel, Switzerland. This article is an open access article distributed under the terms and conditions of the Creative Commons Attribution (CC BY) license (https://creativecommons.org/licenses/by/4.0/).

1. Introduction

Lever mechanisms have been used to amplify force or displacement for a mechanical advantage since time immemorial. Based on the conservation of energy, the amount of amplification a lever provides can be calculated as the ratio of the distance from the pivot point to the effort point and that from the pivot point to the load point. Numerous mechanical mechanisms and devices have been developed successfully with proper lever mechanisms [1–6]. H. Lin and W. Feng proposed a torque generator-driven lever mechanism for a torsional mirror. In the mechanism, a lever was exploited to enlarge traveling distance in limited design space [1]. Woude et al. developed a new design for a lever-propelled wheelchair [2]. K. Li and M. Gohnert suggested a lever mechanism for improving vibration isolation performance. In their study, damping force was conveyed to the mass through the lever [3]. Several researchers have developed gripper mechanisms for microelectromechanical systems (MEMS) using lever mechanisms. C. Shi et al. proposed a microgripper with a large magnification ratio. In this mechanism, the lever successfully amplified the limited output displacement of a lead zirconate titanate (PZT) actuator for the desired displacement of the gripper [4]. K. Kwon et al. developed a linear motor using a lever mechanism to improve the position accuracy. Unlike this mechanism of a microgripper, the lever mechanism in a linear motor had the role of reducing the displacement [5]. M. French and M. Widden developed a static balancing mechanism using a spring and lever. In this mechanism, the lever amplified the spring force and achieved a lightweight static balancer for a lamp [6].

In recent years, lever mechanisms with variable amplification ratios have frequently been applied in robot mechanisms, particularly variable stiffness actuators [7–12]. A. Jafari et al. [7] and N. Tsagarakis [8] et al. proposed adjustable stiffness actuators with class 1 levers for ankle assistance mechanisms. Sun et al. [10], Groothuis et al. [11] and Barrett et al. [12] also developed a class 1 lever-based actuator to achieve variable stiffness. To adjust the stiffness, the lever position was varied using an additional motor. B. Kim and

J. Song also developed a variable stiffness actuator with a lever mechanism. When the class 2 lever mechanism was applied, the position of the lever's load point varied to change the actuator's stiffness [9]. Although the lever mechanisms with a variable amplification ratio achieved the desired function successfully, the shape for the levers was a straight line. Moreover, due to the simplicity of the straight lever, the above-mentioned studies did not propose a lever contour design methodology.

However, when a lever had an additional required function beyond amplification such as preventing intervention between design spaces or maximizing the variable range of amplification ratio, the lever was required to have a shape other than a simple straight line. J. Kim et al. developed a compact variable gravity compensation mechanism with a non-straight lever shape. An angled lever was devised to achieve the amplification of the spring force and also to satisfy the circular design space, [13]. M. Dezman and A. Gams suggested an arc-shaped lever-based compliant actuator to satisfy both force amplification and energy-efficient stiffness variation functions [14]. Although these studies showed a non-straight lever shape, the geometries of the levers' contours were still simple and did not require any particular contour design methodology.

J. Kim et al. [15] proposed a curved lever design to improve the performance of a variable gravity compensation mechanism. In this method, the curved lever was mathematically modeled based on B-spline representation and optimized using a genetic algorithm. Although the research suggested a curved lever design methodology, there was a limitation that the lever contour was represented as a unitary curve. This approach is suitable for a nonfunctional lever contour. However, when a multifunctional lever contour is designed using a unitary curve model and optimization approach, the complexity of the design problem could worsen due to the difficulties of determining the design vector and constructing a multivariable objective function with weighting factors.

Recently, we proposed a new version of a compact variable gravity compensator with a multifunctional lever [16]. In this study, first, we proposed the early concept of divide-and-conquer design methodology for a curved lever contour. Although the lever contour, on the paper, showed the potential of the divide-and-conquer design methodology, one of the lever contours still had a curve representation for two assigned functions. When the lever contour was optimized for two variable objective functions, design variables that maximize each function could not be selected.

To overcome the limitation of the above-mentioned lever contour design methods, in this study, we proposed a bioinspired divide-and-conquer design methodology for multifunctional lever contours. *Salvia pratensis* flowers have a curved lever mechanism in the staminal lobe as an effective pollen dispensing system. The staminal lever curve can be subdivided into a contour to prevent interference with bees' heads and a contour for applying pollen to bees' abdomens. From this morphological insight, we subdivided all required functions into subfunctions that were assigned to the design goal of each partial contour. Each contour was represented by a mathematical curve model suitable for achieving the assigned function and was determined through an appropriate method. The design methodology provides a design tool for the designer to generate a multifunctional lever contour.

To convey the usage of the methodology, we determined the compact variable gravity compensation (CVGC) mechanism as a design case study. Four subfunctions were assigned to the curved lever, which included: (1) minimizing the required force for the torque variation, (2) maximizing the variable range of the compensation torque, (3) preventing interference with cam structure, and (4) connecting between contours with C1 continuity. The experiments showed that the derived lever contour successfully achieved all subfunctions simultaneously. Moreover, the lever contour showed a 1.3 times wider variable range as compared with the lever in [16]. This paper is organized as follows: In Section 2, we explain the bioinspired insight from *Salvia pratensis* flowers and the concept of the lever contour design methodology in detail; in Section 3, we describe the operating concept of CVGC and the required functions for the curve lever mechanism; in Section 4, we discuss the detailed

design processes for the lever contour; in Section 5, we show the experimental results of the designed curved lever contour; and finally, in Section 6, we present our conclusions.

2. Bioinspired Curved Lever Contour Design Methodology

Divide-and-conquer design methodology for the multifunctional contour of the curved lever was developed, inspired by a staminal lever system of the *Salvia pratensis* flower. To convey the bioinspired features of the methodology, the morphological characteristics of the staminal lever are illustrated in Section 2.1. In Section 2.2, the design methodology is explained in detail.

2.1. Curved Lever Mechanism in Salvia pratensis Flower

The *Salvia pratensis* flower has a staminal lever system that can dispense pollen to flower-visiting bees' abdomens for successful reproduction [17]. As shown in Figure 1a, the lever system is composed of a connective plate, a fertile anther lobe, and a rotational joint that has the role of a pivot. When a bee pushes its proboscis into the flower, the connective plate is forced to the left, as in Figure 1a. This force rotates the connective plate and fertile anther lobe clockwise. Therefore, the theca placed at the end of anther lobe makes contact with the bee's abdomen.

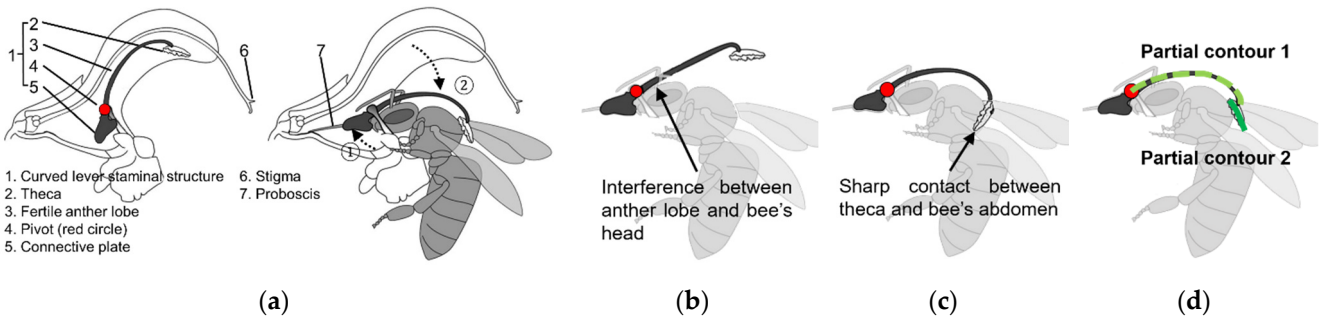


Figure 1. Schematic drawing of the lever mechanism in a *Salvia pratensis* flower and its interaction with a flower-visiting bee as depicted by Reith et al. [17]: (**a**) Longitudinal section of a flower and motions of the curved staminal lever; (**b**) a hypothetical straight-line staminal lever; (**c**) a hypothetical staminal lever where the theca has the same curvature as the anther lobe; (**d**) a real staminal lever composed of two partial contours. The partial contours 1 and 2 prevent interference with the bee's head and avoid sharp contact between the theca and the bee's abdomen, respectively.

The contour of the lever has a proper curved shape to achieve the successful dispensing of pollen. As shown in Figure 1b, if the contour of an anther lobe was a straight line, the theca could not make contact with a bee's abdomen due to interference with the bee's head. In addition, if the contour of the theca had the same curvature as the anther lobe shown in Figure 1c, the theca would make sharp contact with the abdomen and fail to dispense pollen effectively due to the narrow contact area.

As illustrated in Figure 1d, the entire lever curve can be seen as a combination of partial contours with individual functional goals. The partial Contour 1 has a proper curve to satisfy the function of preventing interference with the bee's head. The partial contour 2 also has a shape that achieves the function of maximizing the contact area between the theca and the bee's abdomen.

2.2. Concept of Bioinspired Design Methodology

As shown in Figure 2, the divide-and-conquer contour design methodology for a multifunctional lever was developed using bioinspired insights. This methodology fundamentally does not treat a lever contour as a single curve that should satisfy multiple functions. Rather, a lever contour is regarded as a combination of partial contours responsible for each subfunction. The procedure for designing a lever with this methodology is as follows: At first, subfunctions should be generated by dividing the overall function. Second, the design space of the lever is also divided into subareas that affect each sub-

function. Third, a partial contour is derived by selecting an appropriate curve expression method and design method in consideration of the assigned subfunctions. Finally, one lever is determined by combining the derived partial contours. The partial contours only consider achieving their own functional goal. Therefore, in this design methodology, the designer can choose the most appropriate mathematical model to represent each partial contour and proper determination method for the design variables of each model. The divide-and-conquer lever design methodology has several advantages as follows: First, it can simplify complex multifunctional design problems.

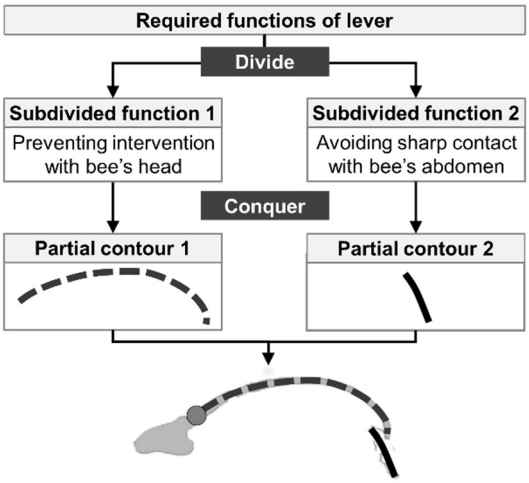


Figure 2. Morphological principle of the staminal curved lever of Salvia pratensis flower. The lever's required functions are subdivided into functions (divide) and assigned to each partial contour as design goals. Each partial contour has a proper shape only to satisfy their subdivided function (conquer). The combination of each partial contour forms the final contour of the curved lever.

A designer can concentrate on designing each partial contour to satisfy relatively simple functional goals. Next, this methodology makes it possible to construct efficient design processes in terms of mathematical modeling and the parameter determination method for each contour. Although some lever design problems may not suit this methodology because the multifunctionality cannot be divided well, the methodology can give a view to simplify the design problem.

3. Curved Lever Contour Design

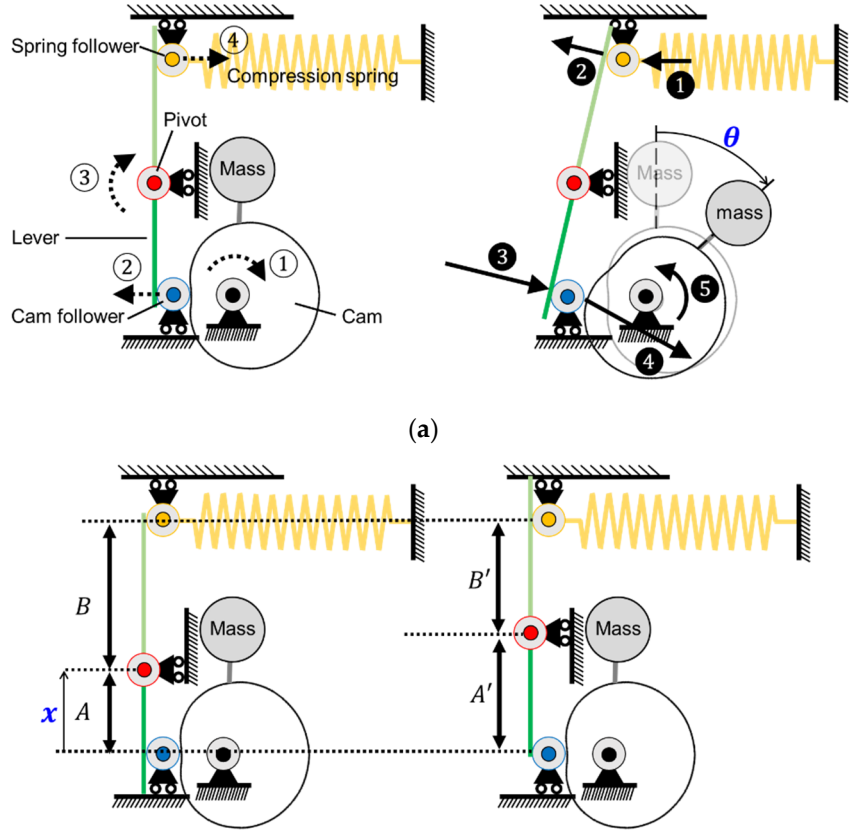
To explain the methodology in more detail, a design case study was conducted for the actual mechanism of CVGC. As the lever mechanism in CVGC should achieve multiple functions, it is an appropriate case to show detailed processes. Before explaining the specific design processes, in this section, we briefly present the operating concept of the CVGC mechanism and the required functions of the lever.

3.1. Operating Concept of the CVGC Mechanism

As a variable gravity compensation mechanism, CVGC could generate compensation torque and change its amplitude to deal with variable gravitational torque. As shown in Figure 3, the core elements of the CVGC mechanism are the cam, cam follower, lever with a movable pivot, spring follower, and compression spring.

Figure 3a illustrates the principle of generating compensation torque. The rotation of an external load, which is the target mass to be compensated, leads to the rotation of the cam. The rotational motion of the cam makes the cam follower move along the linear guide and the movement of the cam follower rotates the lever clockwise about the pivot axis. This rotation of the lever pushes the spring follower to the right and compresses the spring. Consequently, the restoration force of the spring compresses the cam follower to

the cam surface. Finally, due to the noncircular cam, the force at the cam surface generates a counterclockwise compensation torque at the cam.



(**a**)

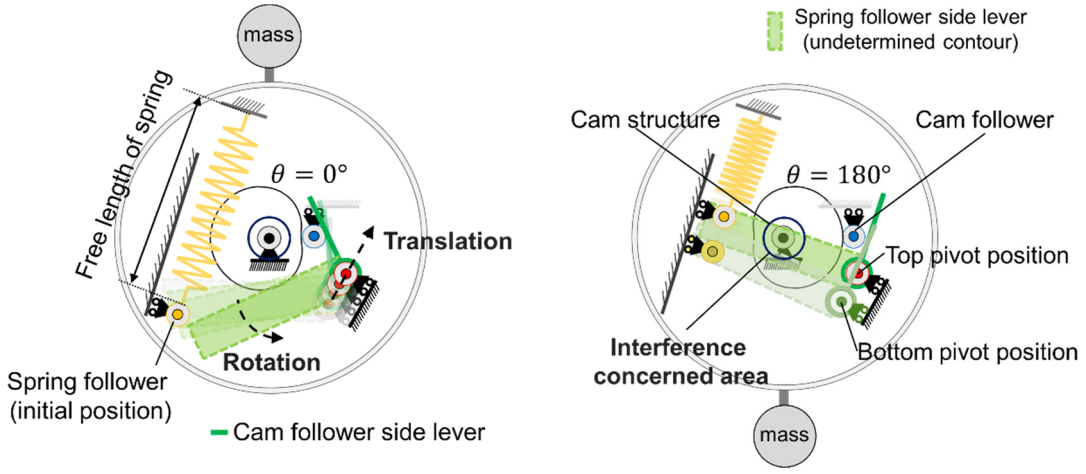
(**b**)

Figure 3. Operating concepts of CVGC for compensating a gravitational torque by mass: (**a**) Configuration and motions of CVGC. The white circled digits indicate the orders of motions describing the spring deformation due to the cam rotation. The black circled digits represent the order of forces that account for the compensating torque in the cam generated by the spring force. θ is the rotation angle of the cam; (**b**) principle of torque variation. The movement of the pivot can change the amplification ratio (B/A or B′/A′). B/A is larger than B′/A′, so it generates a larger compensation torque at the cam axis, and x denotes the distance between pivot position and cam follower.

Figure 3b illustrates the principle of compensation torque variation. The lever mechanism in CVGC can change its pivot position and the amplification ratio. Changing the ratio makes the magnitude of the force and the compensation torque generated on the cam controllable.

3.2. Three Types of Functional Requirements of Levers for CVGC

According to the abovementioned principles, the CVGC mechanism has been developed to achieve a compact and circular shape as shown in Figure 4. The lever has the role of amplifying the spring force and transmitting it to the cam in the limited design space. To maximize the performance of CVGC, the multiple functions that the lever should satisfy are: (1) minimizing the required force of the torque variation, (2) maximizing the variable range of the compensation torque, and (3) avoiding interference between the lever and other mechanical elements.



(**a**) (**b**)

Figure 4. Functional requirements of the lever for CVGC: (**a**) The translation and rotation of the lever when the pivot position changes; (**b**) the maximum compressions of the spring at each top pivot position and bottom pivot position. Interference can occur between the lever and cam structure.

For the first function, minimizing the required force for the torque variation is essential to achieve high energy efficiency in the variable mechanism. When the variation is automated by an actuator, a large force is required which increases the actuator's size and weight and decreases the energy efficiency. Since the fundamental goal of CVGC is to create a compact mechanism, the first function should be satisfied by the lever design. The required force to change the pivot position can be calculated by the Lagrangian mechanics as follows:

$$F_{variation}(x) = -\frac{\partial PE_{spring}(x)}{\partial x} \quad (1)$$

x, $PE_{spring}(x)$, and $F_{variation}(x)$ denote the generalized coordinates, the force, and potential energy profile of the mechanism, respectively.

According to (1), if the energy variation is zero with respect to the change of pivot position, the required force can be zero in ideal frictionless conditions. The amount of spring deformation can be determined by the position of the spring follower. As shown in Figure 4, the rotation and translation of the lever occur simultaneously when the pivot changes. From the lever design perspective, the lever contour should not change the position of the spring follower when the pivot position varies.

Next, the second function of the lever is important because a wide variable range of compensation torque obviously allows CVGC to compensate for variable weight. The variable range of the compensation torque is calculated as the difference between the highest and lowest compensation torques. As illustrated in Figure 4b, for the CVGC mechanism that varies the compensation torque by changing the pivot position, it generates the highest torque when the pivot is placed at the top position of the pivot guide and generates the lowest torque when the pivot is placed at the bottom position.

According to [15], the maximum deformations of the spring at each pivot position of the CVGC mechanism could determine the amount of compensation torque. Therefore, to maximize the variable range of the torque, the lever contour should maximize the spring's deformation at the top pivot position as this is directly related to the highest torque. At the same time, this contour should minimize the spring's deformation at the bottom pivot position to minimize the lowest compensation torque. The design point to be considered in this process is that this lever contour must not compress the spring beyond its allowable deformation length.

As a final function of a lever, the lever contour should be designed to prevent interference with other mechanical elements. In particular, the cam structure, including the

cam, camshaft, and bearings, is the main obstacle that hinders the lever from pressing the spring follower sufficiently. For the CVGC mechanism, the worst condition causing an interference problem between the lever contour and the cam structure is when the cam rotates 180° at the top pivot position. Therefore, as shown in Figure 4b, designing the lever contour to avoid interference at this worst condition is sufficient to prevent interference at other pivot positions.

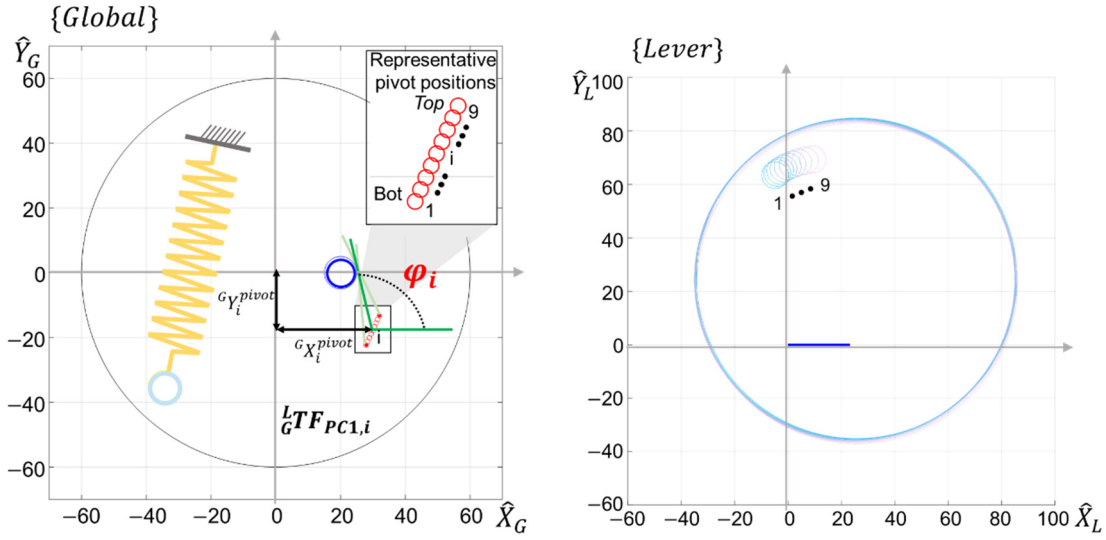
4. Curved Lever Contour Design

To design the lever contour to achieve the multifunctionality mentioned in Section 3.2, the divide-and-conquer design methodology is applied. Through this method, each sub-function is assigned to the design goal of each partial contour. Partial contours are separately designed to satisfy their individual goals, and then combined as a final lever contour.

The geometrical design parameters of other mechanical components such as the cam profile, cam follower guides, and spring follower are given as geometrical constraints that those should not be able to pass through. The shape of the lever can be divided into the cam follower side and spring follower based on the pivot. In this section, it is assumed that the lever contour of the cam follower side is predetermined as a straight line and aims to design only the contour on the spring follower side.

4.1. Partial Contour 1 (PC1): Minimizing the Required Force for Torque Variation

The PC1 should not change the position of the spring follower when the pivot position varies along the pivot guide. The CVGC varies the compensation torque when the rotation angle of the cam is zero. Since the cam follower side of the lever always contacts the cam follower, the translation and rotation of the lever occur simultaneously when the pivot position changes, as illustrated in Figure 5a.



(**a**) (**b**)

Figure 5. *Cont.*

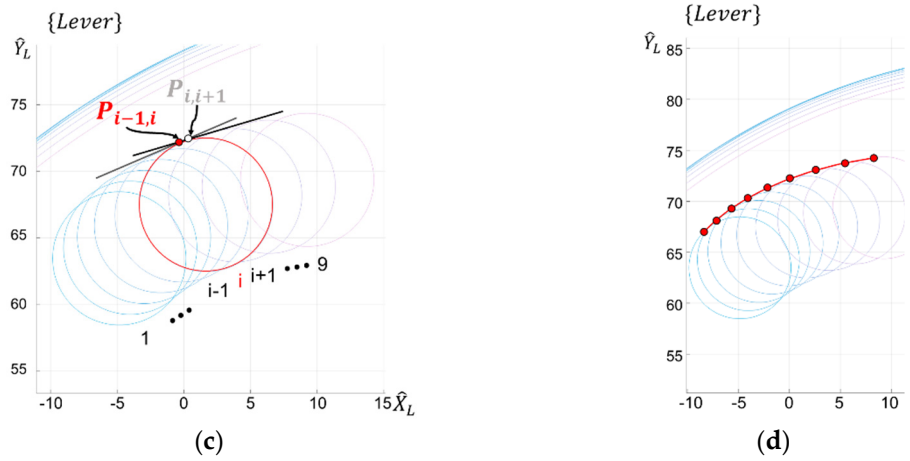


Figure 5. Design processes of the PC1. The units of *x*- and *y*-axes are mm: (**a**) Parameters to calculate transformation matrices at each representative pivot position; (**b**) spring followers are represented in the lever coordinate system; (**c**) common circumferential lines and points and principle to choosing the representative contact points; (**d**) the representative contact points of each spring follower and Hermite spline-based PC1.

In a global coordinate system, the contour design is complex due to the changes of relative angles and distances between the lever and the spring follower. However, the positions of points that determine the rigid lever shape do not change in the lever coordinate system. Therefore, the lever design problem can become easier when in a lever coordinate system.

To calculate the coordinate transformation, representative pivot positions are determined by dividing the pivot guidelines equally into n sections. Nine representative pivot positions were selected, including the top and bottom pivot positions. The unit length for a section and the rotation angles at each pivot position can be determined using (2) and (3) as follows:

$$D_x = \frac{{}^{G}X_9^{pivot} - {}^{G}X_1^{pivot}}{8}, \; D_y = \frac{{}^{G}Y_9^{pivot} - {}^{G}Y_1^{pivot}}{8} \tag{2}$$

$$\varphi_i = \frac{\pi}{2} + \sin^{-1}\frac{r_{cam}}{B_i} \tag{3}$$

where ${}^{G}X_i^{pivot}$ and ${}^{G}Y_i^{pivot}$ indicate the position of the i^{th} pivot in the global coordinates; D_x and D_y are the x and y components of the unit length, respectively; r_{cam} is the radius of the cam follower. Then, the translation and transformation matrices at the i^{th} selected pivot positions can be calculated using (4) and (5), respectively, as follows:

$$\begin{bmatrix} {}^{G}X_i^{pivot} \\ {}^{G}Y_i^{pivot} \end{bmatrix} = \begin{bmatrix} {}^{G}X_1^{pivot} + (i-1)D_x \\ {}^{G}Y_1^{pivot} + (i-1)D_y \end{bmatrix} \tag{4}$$

$${}^{L}_{G}TF_{PC1,i} = \begin{bmatrix} C_{-\varphi_i} & -S_{-\varphi_i} & 0 & -{}^{G}X_i^{pivot} \\ S_{-\varphi_i} & C_{-\varphi_i} & 0 & -{}^{G}Y_i^{pivot} \\ 0 & 0 & 1 & 1 \\ 0 & 0 & 0 & 1 \end{bmatrix} \tag{5}$$

where the left subscript G in (4) is the lever and global coordinate system, the left subscript G and the superscript L represent the global coordinates and lever coordinates, respectively, and C and S are the cosine and sine, respectively.

Using the transformation matrices, the fixed spring follower positions are transformed into a lever coordinate system and nine circles are generated, as shown in Figure 5b. The PC1 should be designed to have a shape that makes contact with all nine circles at the same time. For the next step, the common circumferential lines and points between adjacent circles are computed to find contact points between the lever and circles. Except for the

first and last circles, the i^{th} circle has two common circumferential lines and contact points between the $i-1^{th}$ and $i+1^{th}$ circles of spring followers. To assign one tangential line and point to a circle, the line and contact point between the $i-1^{th}$ circle are selected. As a result, each of the nine circles has a corresponding contact point and slope of the tangential line at that point, as illustrated in Figure 5c.

For the last step, piecewise curves connecting to the adjacent contact points with a satisfactory slope are generated based on the third order Hermite spline. Consequently, the PC1 is formed by connecting the eight piecewise curves that enable tangential contact with the spring follower at each pivot position, thereby achieving subfunction 1 as shown in Figure 5d.

4.2. Partial Contour 2 (PC2): Maximizing the Variable Range of the Compensation Torque

A B-spline curve representation and optimization approach is adopted to generate a PC2 that satisfies the subfunction. As illustrated in Figure 6a, five control points are placed in the lever coordinates system to form a B-spline curve of PC2. The start and end points among the five control points are determined by an obstacle point and a connecting point, respectively, as explained in detail later. A serial link representation is used to avoid the cusp issue [15] as in (6)–(15) as follows:

$$^{L}CP_{0x} = Px_{obstacle} \tag{6}$$

$$^{L}CP_{0y} = Py_{obstacle} \tag{7}$$

$$^{L}CP_{4x} = Px_{connecting} \tag{8}$$

$$^{L}CP_{4y} = Py_{connecting} \tag{9}$$

$$^{L}CP_{1x} = G_1C_{\Theta_1} + G_2C_{\Theta_1+\Theta_2} \tag{10}$$

$$^{L}CP_{1y} = G_1S_{\Theta_1} + G_2S_{\Theta_1+\Theta_2} \tag{11}$$

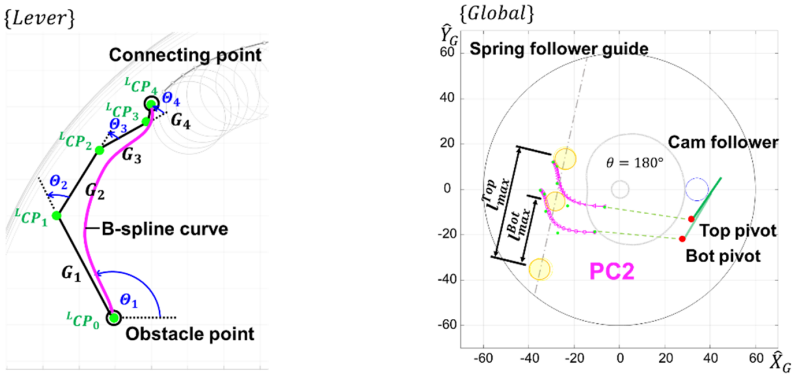
$$^{L}CP_{2x} = G_1C_{\Theta_1} + G_2C_{\Theta_1+\Theta_2} + G_3C_{\Theta_1+\Theta_2+\Theta_3} \tag{12}$$

$$^{L}CP_{2y} = G_1S_{\Theta_1} + G_2S_{\Theta_1+\Theta_2} + G_3S_{\Theta_1+\Theta_2+\Theta_3} \tag{13}$$

$$^{L}CP_{3x} = {}^{L}CP_{2x} + G_4C_{\Theta_1+\Theta_2+\Theta_3+\Theta_4} \tag{14}$$

$$^{L}CP_{3y} = {}^{L}CP_{2y} + G_4S_{\Theta_1+\Theta_2+\Theta_3+\Theta_4} \tag{15}$$

where G_i is the length of the i^{th} link and Θ_i is the relative angle between the $i-1^{th}$ and i^{th} link.



(**a**) (**b**)

Figure 6. Design of the PC2. The unit of the x- and y-axes are mm: (**a**) B-spline modeling to design PC2 using optimization; (**b**) maximum compression of the spring at each top and bottom pivot position, which constitute the objective function.

The objective function for optimizing the B-spline is defined to maximize the variable range of the compensation torque as follows:

$$g(q) = \frac{l_{max}^{Top}}{l_{max}^{Bot}} \tag{16}$$

l_{max}^{Top} and l_{max}^{Bot} are the maximum deformation of the spring when the pivot is placed at the top and bottom positions, respectively, as shown in Figure 6b. The denominator of the objective function increases as the deformation of the spring at the bottom pivot position decreases, which is related to the lowest compensation torque. The numerator increases when the deformation of the spring at the top pivot position increases, which is related to the highest compensation torque. The case in which the deformation by the PC2 exceeds the allowable deformation of the spring is excluded as a constraint condition. Therefore, the larger the objective function, the larger the variable range of the compensation torque that can be acquired.

Since l_{max}^{Top} and l_{max}^{Bot} can be calculated by the geometrical relation between the B-spline curve and the spring follower guideline, the lever contour defined in the lever coordinate system should be transformed to the global coordinate system. Consequently, the optimization problem is as follows:

$$\begin{gathered} Given\ q = [G_1, \Theta_1, G_2, \Theta_2, G_3, \Theta_3] \\ maximize\ g(q) \end{gathered} \tag{17}$$

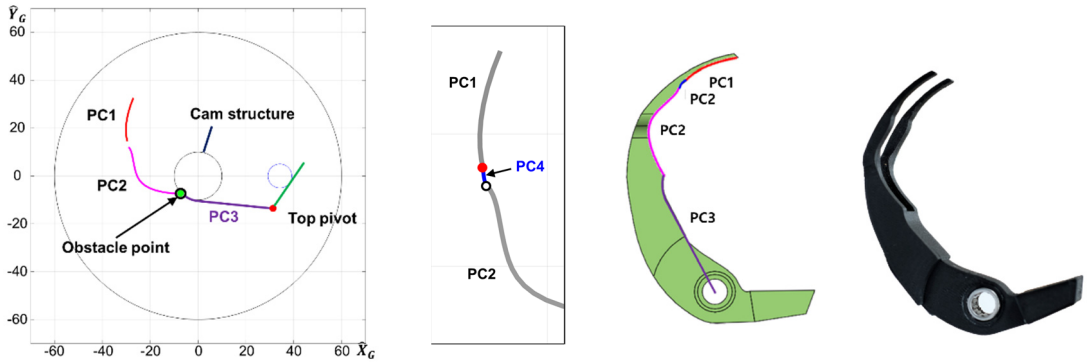
Table 1 shows the optimization result computed by the genetic algorithm in the global optimization toolbox of MATLAB (MATLAB R2019b, MathWorks, United States). The optimal PC2 generates 50.4 mm and 29.8 mm as the maximum compression lengthx of the spring at the top and bottom pivot positions, respectively.

Table 1. Optimal design variables of PC2.

Pivot	CP_1	CP_2	CP_3
G (m)	0.0162	0.0107	0.0076
Θ (°)	119.5	−62.03	−26.28

4.3. Partial Contour 3 (PC3): Preventing Interference with the Cam Structure

As shown in Figure 4B, the PC3 should be designed to avoid interference with the cam structure only when the cam rotates to 180° at the top pivot position. As illustrated in Figure 7, in the global coordinate system, the common circumferential line and points between the circle of the cam structure and the highest spring follower can be calculated.



(**a**) (**b**) (**c**) (**d**)

Figure 7. (**a**) Design of PC3 to avoid interference with the cam structure. The units of *x*- and *y*-axes are m; (**b**) design of PC3 to secure C1 continuity between PC1 and PC2; (**c**) final lever contour combining partial contours; (**d**) manufactured lever contour.

The common point on the circle of the cam structure is the obstacle point that is used to design PC2. The obstacle points allow PC2 to avoid interference with the cam structure. Considering that the mass of the lever is proportional to its length, PC3 is determined using the simplest straight line and arc, as illustrated in Figure 7a.

4.4. Partial Contour 4 (PC4): Connecting PC1 and PC2 with C1 Continuity

As a final step of the divide-and-conquer design methodology, combining the derived partial contours with proper continuity condition is important to generate the final contour. The connection between PC2 and PC3 is the area in which the spring follower does not contact with the spring follower. Therefore, the C0 continuity is sufficient to combine the PC2 and PC3. However, the area between the PC1 and PC2 makes contact with the spring follower, so the connection should satisfy the C1 continuity to ensure the smooth motion of the spring follower.

To achieve the connection with C1 continuity, PC4 is designed as follows: On the PC1 side, the starting point and slope at that point are already determined, as described in Section 4.1.

The starting point of PC1 extends by distance ε in the direction of the slope to make the connecting point. The connecting point is used as the fifth control point of PC2, as described in Section 4.2. Using the partial derivatives of PC2, the slope at the connecting point can also be calculated. Finally, based on the Hermite spline representation, PC4 can be determined, as illustrated in Figure 7b. A pseudo code of the algorithm for the design of partial contours is attached in Supplementary Materials.

5. Experiments and Results

The detail design of the lever contour made by combining PC1, PC2, PC3, and PC4 is as presented in Figure 7c. To verify that the lever achieves the desired multifunctions, experiments are separately conducted on each partial contours. As shown in Figure 7d, the lever used in the experiments was manufactured with a 3D-printer (Mark Two, Mark-forged, MA, US) with carbon-fiber materials that have sufficient strength for experimental verifications. According to the visual measurement method, the experiments successfully checked that each partial contour satisfied the geometrical conditions to achieve a given subfunction. Figure 8 illustrates the manufactured CVGC mechanism with the designed lever contour.

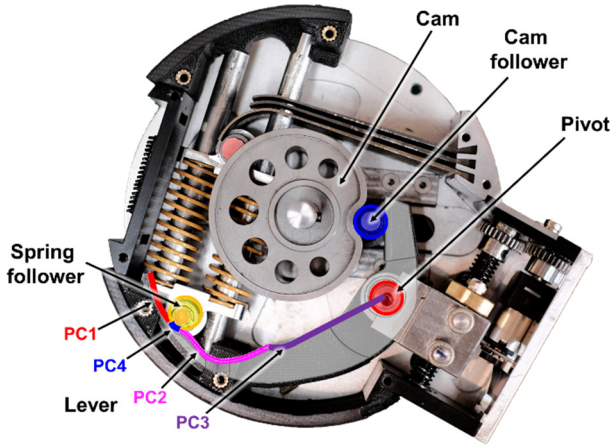


Figure 8. Manufactured CVGC mechanism with the designed lever contour.

To verify the subfunction of PC1, the position of the spring follower was measured by marker tracking when the position of the pivot changed. Although a minor position. change of the spring follower occurred, PC1 successfully minimized the movement, as shown in Figure 9.

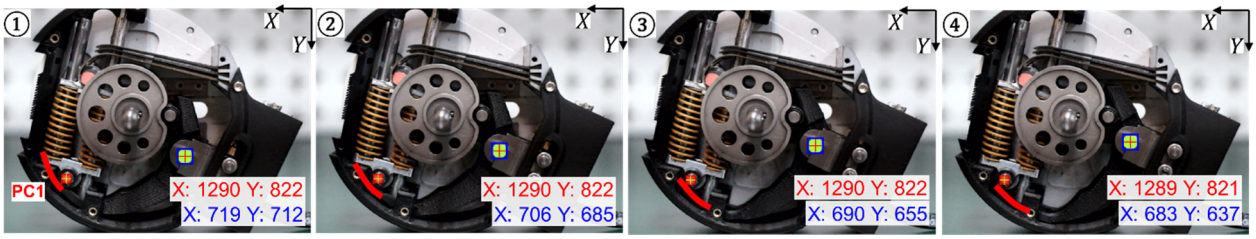


Figure 9. The visual measurement to verifying PC1 using marker tracking. The red and blue coordinates indicate the position of the spring follower and the pivot position with respect to the origin at the right top of the figure. The circled numbers show the order of pivot variation from the bottom pivot (circled number 1) to the top pivot (circled number 4). The total travel distance of the pivot is 10 mm. Through the proper design of PC1, the position of the spring follower does not be affected by the movement of the pivot.

The position change of the spring follower had 0.4 mm as its maximum value. The reason for the design error of PC1 is the lack of a number of representative pivot points; therefore, this error can be mitigated by increasing the number of representative pivot points and piecewise curve segments of PC1.

Next, each position of the spring follower was measured at the top and bottom pivot positions to verify the function achievement of PC2. As presented in Figure 10 and Table 2, the amounts of spring deformation at each pivot condition are 29.5 and 50.5 mm, which is well-matched with the designed values. The errors of deformation length between simulation and experiment are 1.0% and 0.1% at the bottom (bot) and top pivot conditions, respectively. The absolute errors are 0.7 and 0.1 mm at the bot and top pivot positions, respectively. We expect the position error of marker installation is the main reason for the errors between simulation and experiment.

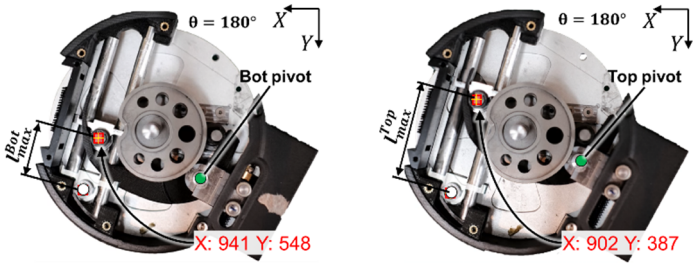


Figure 10. The visual measurement to verifying PC2 using marker tracking. The maximum deformations of the spring at the bot pivot and top pivot conditions are shown in the left and right figures. The red coordinates information indicates the position of the spring follower.

Table 2. Comparison of simulation and experimental results for the maximum deformation of spring at the top and bottom pivot conditions.

Maximum Deformation	Simulation	Experiment
l_{max}^{Bot}(mm)	29.8	29.5
l_{max}^{Top}(mm)	50.4	50.5

Finally, to verify the interference avoidance in the lever and cam structure, which is a function of PC3, the lever was observed at the top pivot position and at 180° cam rotation. As shown on the right side of Figure 10, the lever pushed the spring follower without any interferences. Therefore, PC3 successfully achieves its subfunction.

6. Conclusions

In this study, we propose a contour design methodology for achieving a multifunctional lever based on the morphological principle of the *Salvia pratensis* flower. In this

methodology, multiple functions were subdivided into subfunctions. Each subfunction was assigned to a partial contour as a design goal. The final lever contour was determined by combining the partial contours that could achieve the given subfunctions. Through this methodology, a designer can simplify complex and multifunctional curve design problems. Moreover, the most suitable modeling and parameters to determine the method can be selected for each partial contour.

This methodology was specifically explained by a design case study of CVGC, in which the lever should achieve three subfunctions. To achieve the first function, PC1 was modeled using a Hermite spline and was directly calculated to find the design parameters. For the second subfunction, PC2 was determined by B-spline model-based optimization. To satisfy the third subfunction, PC3 was derived simply by using an arc and straight line model. In addition, the PC4 based on Hermite spline was designed to generate a smooth rolling contact with the spring follower.

Finally, through marker tracking-based visual verification, it was verified that, for the derived lever contour, each partial contour could successfully achieve subfunctions. PC1 did not change the position of the spring follower and did not generate deformation of the compression spring. The difference between the maximum deformation of the spring was increased 1.3 times by PC2 when the pivot was placed in the top and bottom (bot) positions as compared with the previously derived lever in [16]. As mentioned in Section 4.2, this difference is directly related to the variable range of compensation torque. PC3 did not prevent any intervention between the lever and cam structure. PC4 achieved C1 continuity between C1 and C2. As future research goals, we plan to install the derived lever into CVGC and measure the performances of the variable gravity compensation torque. In addition, we are developing various versions of CVGC with different sizes and compensation torques. Therefore, we will actively utilize this methodology to design various versions of levers.

Supplementary Materials: The following are available online at https://www.mdpi.com/article/10.3390/app11136015/s1, Figure S1: Pseudo code of the algorithm for the design lever contours for the CVGC case study.

Author Contributions: Conceptualization, J.K., J.M., J.R. and G.L.; methodology, J.K., J.M. and G.L; software, J.K., J.M. and G.L.; validation, J.M., J.R. and G.L.; data analysis, J.K., J.R. and G.L.; writing—original draft preparation, J.K. and G.L.; writing—review and editing, J.K. and G.L.; visualization, J.K. and G.L.; supervision, J.M. and G.L.; project administration, G.L.; funding acquisition, G.L. All authors have read and agreed to the published version of the manuscript.

Funding: This research was funded by the Samsung Research Funding & Incubation Center of Samsung Electronics under Project Number SRFC-IT1903-02 and supported by the Chung-Ang University Research Grants in 2021.

Institutional Review Board Statement: Not applicable.

Informed Consent Statement: Not applicable.

Data Availability Statement: Not applicable.

Conflicts of Interest: The authors declare no conflict of interest.

References

1. Lin, H.; Fang, W. Torsional mirror with an electrostatically driven lever-mechanism. In Proceedings of the 2000 IEEE/LEOS International Conference on Optical MEMS, Kauai, HI, USA, 21–24 August 2000; pp. 113–114.
2. Van der Woude, L.H.V.; Veeger, H.E.J.; de Boer, Y.; Rozendal, R.H. Physiological evaluation of a newly designed lever mechanism for wheelchairs. *J. Med. Eng. Technol.* **1993**, *17*, 232–240. [CrossRef] [PubMed]
3. Li, K.; Gohnert, M. Lever mechanism for vibration isolation. *Appl. Technol. Innov.* **2010**, *1*, 21–28. [CrossRef]
4. Shi, C.; Dong, X.; Yang, Z. A Microgripper with a Large Magnification Ratio and a High Structural Stiffness Based on a Flexure-Enabled Mechanism. *IEEE/ASME Trans. Mechatron.* **2021**. early access. [CrossRef]
5. Kwon, K.; Cho, N.; Jang, W. The design and characterization of a piezo-driven inchworm linear motor with a reduction-lever mechanism. *JSME Int. J. Ser. C* **2004**, *47*, 803–811. [CrossRef]

6. French, M.J.; Widden, M.B. The spring-and-lever balancing mechanism, George Carwardine and the Anglepoise lamp. *Proc. Inst. Mech. Eng. Part C J. Mech. Eng. Sci.* **2000**, *214*, 501–508. [CrossRef]
7. Jafari, A.; Tsagarakis, N.G.; Sardellitti, I.; Caldwell, D.G. A new actuator with adjustable stiffness based on a variable ratio lever mechanism. *IEEE/ASME Trans. Mechatron.* **2012**, *19*, 55–63. [CrossRef]
8. Tsagarakis, N.G.; Sardellitti, I.; Caldwell, D.G. A new variable stiffness actuator (CompAct-VSA): Design and modelling. In Proceedings of the 2011 IEEE/RSJ International Conference on Intelligent Robots and Systems, San Francisco, CA, USA, 25–30 September 2011; pp. 378–383.
9. Kim, B.; Song, J. Hybrid dual actuator unit: A design of a variable stiffness actuator based on an adjustable moment arm mechanism. In Proceedings of the 2010 IEEE International Conference on Robotics and Automation, Anchorage, AK, USA, 3–7 May 2010; pp. 1655–1660.
10. Sun, J.; Guo, Z.; Zhang, Y.; Xiao, X.; Tan, J. A novel design of serial variable stiffness actuator based on an archimedean spiral relocation mechanism. *IEEE/ASME Trans. Mechatron.* **2018**, *23*, 2121–2131. [CrossRef]
11. Groothuis, S.S.; Rusticelli, G.; Zucchelli, A.; Stramigioli, S.; Carloni, R. The Variable Stiffness Actuator vsaUT-II: Mechanical Design, Modeling, and Identification. *IEEE/ASME Trans. Mechatron.* **2014**, *19*, 589–597. [CrossRef]
12. Barrett, E.; Fumagalli, M.; Carloni, R. Elastic Energy Storage in Leaf Springs for a Lever-Arm Based Variable Stiffness Actuator. In Proceedings of the 2016 IEEE/RSJ International Conference on Intelligent Robots and Systems (IROS), Daejeon, Korea, 9–14 October 2016; pp. 537–542.
13. Kim, J.; Moon, J.; Kim, J.; Lee, G. Design of Compact Variable Gravity Compensator (CVGC) Based on Cam and Variable Pivot of a Lever Mechanism. In Proceedings of the 2019 IEEE/RSJ International Conference on Intelligent Robots and Systems (IROS), Macau, China, 3–8 November 2019; pp. 3583–3588.
14. Dežman, M.; Gams, A. Pseudo-linear variable lever variable stiffness actuator: Design and evaluation. In Proceedings of the 2017 IEEE International Conference on Advanced Intelligent Mechatronics (AIM), Munich, Germany, 3–7 July 2017; pp. 785–790.
15. Kim, J.; Moon, J.; Kim, J.; Lee, G. Compact Variable Gravity Compensation Mechanism with a Geometrically Optimized Lever for Maximizing Variable Ratio of Torque Generation. *IEEE/ASME Trans. Mechatron.* **2020**, *25*, 2019–2026. [CrossRef]
16. Kim, J.; Moon, J.; Ryu, J.; Lee, G. CVGC-II: A new version of a compact variable gravity compensator (CVGC) with a wider range of variable torque and an energy-free variable mechanism. *IEEE Trans. Mechatron.* accepted.
17. Reith, M.; Baumann, G.; Claßen-Bockhoff, R.; Speck, T. New insights into the functional morphology of the lever mechanism of *Salvia pratensis* (Lamiaceae). *Ann. Bot.* **2007**, *100*, 393–400. [CrossRef] [PubMed]